applied sciences

MDPI

Article

Print Quality Analysis of Stone Paper and Coated Sticker Paper Used in Screen Printing

Cem Akpolat [1,*] and Ahmet Akgül [2]

[1] Department of Printing and Publishing Technologies, Kayseri University, 38280 Kayseri, Türkiye
[2] Department of Printing Technologies, Faculty of Applied Sciences, Marmara University, 34722 Istanbul, Türkiye; ahmetakgul@marmara.edu.tr
* Correspondence: cemakpolat@kayseri.edu.tr

Abstract: The sustainable use of natural resources is becoming an increasingly important issue today. Stone paper, produced as an alternative to cellulose-based paper from the forest, is rich in minerals and produced without cellulose and water. This study focuses on the behavior of screen-printing ink on two different papers, stone paper and coated sticker paper. Properties such as ink adhesion, rubbing resistance, optical printing ink density, ink consumption, and lightfastness were measured on these surfaces. Solvent- and UV-based inks were used, and printing was carried out on cellulose-based (coated sticker paper) and mineral-based (stone paper) paper layers using three different mesh counts (90, 120, and 140 tpc). The rubbing resistance and lightfastness of the papers were also measured. The present findings revealed that stone paper had the same printability properties as cellulose-based paper. The study concluded that using a 140 tpc mesh with both types of ink results in a high-lightfastness ink layer and lower ink consumption. UV-based inks exhibited high rub resistance across all mesh counts. Additionally, when printing with stone paper, there will be a reduction in ink consumption, thereby achieving cost savings. Based on the present findings, it was concluded that water- and oil-resistant stone paper can be considered an essential alternative in many fields, including the printing industry.

Keywords: stone paper; lightfastness; rub resistance; screen printing; printability; printing substrate

Citation: Akpolat, C.; Akgül, A. Print Quality Analysis of Stone Paper and Coated Sticker Paper Used in Screen Printing. *Appl. Sci.* **2024**, *14*, 6668. https://doi.org/10.3390/app14156668

Received: 3 June 2024
Revised: 8 July 2024
Accepted: 16 July 2024
Published: 30 July 2024

1. Introduction

Screen printing has quite a broad range of applications compared to other printing techniques. It offers a wide range of applications, from the printing industry to billboards; from printing on industrial products such as bottles, tubes, and glasses to printing on textile products; and from printing electronic circuit boards to producing solar panels and printing on ceramic surfaces [1,2]. The advantages of screen printing are that ink can be controlled and the desired saturation levels can be achieved. It also allows printing on surfaces that cannot be printed on with other printing techniques [3–5].

The printing industry is the primary application area for screen printing. In the printing industry, "stone paper", which addresses the same field as cellulose-based paper, is also used. Stone paper, also referred to as rock paper or rich mineral paper, has some superior properties; for instance, water is not used in stone paper production, and it can be produced without using wood cellulose like conventional paper. It allows for environmentally friendly production since it does not consume water and cellulose, which are natural resources [6]. Calcium carbonate ($CaCO_3$) is the primary raw material of stone paper and is abundantly available in nature [7,8]. In general, the natural formation of $CaCO_3$ involves the process of calcium and carbonate ions being dissolved in water, coming together, and precipitating through combining. This process usually begins with the production and accumulation of $CaCO_3$ by marine organisms, also called biomineralization. Over time, these sedimentation and accumulation processes can form large limestone

deposits and other $CaCO_3$ derivatives [9,10]. Stone paper comprises a combination of powdered inorganic minerals, high-density polyethylene (HDPE) plastic, and additives. Inorganic minerals are materials used like fibres in traditional paper.

Meanwhile, HDPE polymer is a binder that holds inorganic minerals together; therefore, a mixture can be formed in a monolayer or composite form [6]. Three processes are used in stone paper production: 1—solvent casting; 2—film blowing extrusion; and 3—casting film extrusion [11]. These production methods are similar to other petroleum resins, such as polypropylene (PP) and polyethylene (PE) [12,13]. For stone paper, whose main compound comes from nature, biodegradable polymers can be used as an alternative to the synthetic resin HDPE used in the production of this paper to dissolve harmlessly in nature [14–16]. In this sense, researchers mainly focus on making stone paper biodegradable, and this area has a patented product [11,17].

This study primarily focuses on printability analyses of stone paper and coated sticker paper with screen printing and their comparisons. Stone paper was selected for its inherent advantages; since it has a polymer structure, it is waterproof and oil-repellent, just like plastic materials, and has a high tear resistance [11]. It is not 100% petroleum resin-like PP, PVC, and HDPE materials; contrarily, it contains 60–81% natural minerals ($CaCO_3$), and the rest is composed of PP, or PE, or HDPE-like polymer resins [6]. Because of these attributes, it is suitable for outdoor use; unlike classical plastics, it contains less polymer resin and is more durable than cellulose-based paper. With these attributes, stone paper can be considered an alternative substrate material for outdoor printing like screen printing. Moreover, "stone paper" can offer an essential alternative for printed electronic products. In a previous study on screen printing, the water-repellent and oil-repellent nature and tear resistance of stone paper were emphasized [18].

Studies on the printability of synthetic papers date back several decades [19]. In a scientific publication on offset printing, it was suggested that stone paper could easily replace uncoated papers in traditional offset printing [20]. Since its invention, stone paper has become commercially available in the form of waterproof books, notebooks, and artist papers. Stone paper magazines, sketchbooks, and plain paper products are manufactured for office printing, writing, artwork, and other practical uses. Notebooks made from stone paper are increasingly being purchased from regular bookstores and stationery suppliers [21]. Similarly, there are printability studies on bio-composite layers produced using polyester resin and epoxy [22,23].

Coated sticker paper was selected in this study since it is a cellulose-based paper frequently preferred in the printing industry. It was also used to compare the behavior of stone paper and coated sticker paper in screen printing.

Screen printing (formerly silk printing) is a stencil process in which ink is transferred to the substrate through a stencil supported by a thin fabric mesh of silk, synthetic fibers, or metal threads stretched tightly over a frame. Pores of silk are occluded in non-image areas and left open in the image area. This image carrier is a so-called mesh. The frame is fed with ink flowing onto the mesh/screen during printing. It is then drawn with a squeegee, which forces the ink through the open pores of the screen. Meanwhile, the substrate is fixed under the screen. It comes into contact with the screen, and the ink is transferred [24]. Screen printing is preferred since a thick layer of ink can be transferred onto a substrate (Figure 1).

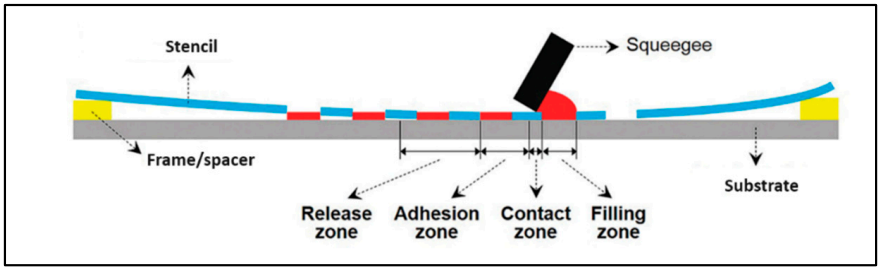

Figure 1. Diagram of screen printing workflow [25].

This feature easily distinguishes screen printing from the other printing techniques; in general, the ink thickness for screen printing is around 20–100 μm, and for offset printing, it is typically around 0.5–2 μm. The thickness of the stencil (the distance at which the stencil rests on the screen) designates the thickness of the ink layer [1].

The factors affecting screen printing quality and their optimization have been researched for several years. Kobs and Voiht conducted a study in 1971; they reported 50 different parameters that affect the quality of screen printing and optimized these parameters. They combined the results of the most critical parameters in 300 different ways [26]. For instance, the squeegee used in print is a parameter; however, changing the drawing pressure of the squeegee during printing or changing its hardness will cause a change in the ink to be transferred onto the substrate material [27,28].

The mesh/screen is the most important factor affecting quality in screen printing since the mesh count determines the rate at which ink is transferred to the substrate. The mesh count and material used in screen printing may vary based on the desired amount of ink to be obtained, the desired characteristics of the image to be printed, and the substrate material to be used. The mesh count refers to the number of threads per centimeter (tpc). Various materials can be stretched over the frame to create the screen printing pattern. Materials such as silk, nylon, monofilament, and multifilament polyester, or metals, are widely used today. Screen printing screens can be produced in 10–200 tpc mesh counts [29]. Screens with a thread count of 200 tpc and above are used for surface printing when more precise patterns are required [3,30]. The distance between the threads increases with decreasing mesh counts, so the amount of ink passing through increases.

On the other hand, the amount of ink passing from the screen to the substrate decreases with increasing mesh counts, but more regular and controlled ink transfer is achieved. Generally, the mesh thread wire diameter decreases or increases proportionally to the mesh count. Wire mesh diameters also affect the amount of ink passing through the mesh [31]. It was indicated in previous studies that the mesh thread count and opening play a key role in determining the amount of ink passing to the substrate, and mesh thread opening is an essential factor in choosing mesh counts [30,32]. Screen printing allows controllable ink transfer; thus, it is frequently used to transition alternative ink types to different printing substrates [33–35].

2. Materials and Methods

Materials

The screens used in this study were made of polyester fabric. They were manufactured by Zhejiang Zhongyi Textile Co., Ltd., Huzhou, Zhejiang, China. The screens were made from monofilament plain weave fabrics and all had the same printing area (10 × 10 cm). For the printing process, a 75° squeegee angle and 3 bar pressure were used for all printing, and a rubber squeegee with 70 Shore A hardness was chosen for printing. The squeegee, with a 15 cm rectangular profile, was obtained from Rakle BMP Europe Ltd., Accrington, UK, and screen tensions were set as 21 N/cm for 120 and 140 tpc screens and 26 N/cm for 90 tpc screens. The reason for the change in mesh tensions is that as the mesh count increases, the wire diameter of the thread used in the mesh decreases, and if the high tension used in a sparse mesh is applied to thin threads and frequent meshes, these screens cannot withstand the high tension and tear [36].

In this study, coated sticker paper of density 80 g/m^2 from Muflon and stone paper of density 240 g/m^2 from Prolux were used as substrate materials. Stone paper (RPD: rich mineral with double-side coating) has a thickness of 200 microns. The technical specifications of the substrates are provided in Table 1, and this information was obtained from the manufacturers. DYO SE-1125-series, cyan-colored, solvent-based ink and TIFLEX-brand, cyan-colored, UV-based ink with reference number 3934000 were used in test printing.

Table 1. Technical specifications for stone paper and coated sticker paper.

		Grammage	Thickness	Density	Whiteness	Opaqueness	Tensile Strength	Thermal Shrinkage	Ultimate Strength
Stone Paper	Test method	CNS 1352 [37]	CNS 3685 [38]	CNS 3685 [38]	CNS 12885 [39]	CNS 14931 [40]	GB 13022-91 [41]	GBT 12027-2004 MD/TD [42]	QB/T 1130-91 MD/TD [43]
	Value	240 g/m^2	200 μm	1.2 g/cm^3	% >86	% >94	>2.5 kg/cm^2	<−2.0% <−4.0%	>0.4% >0.5%
Coated Sticker Paper	Test method	ISO 536 [44]	ISO 534 [45]	-	D65 ISO 2470-2 [46]	-	ISO 1924-3 MD/TD [47]	-	-
	Value	80 g/m^2	70 μm	N.A.	90%	N.A.	69 (−10) N/15 mm 39 (−7) N/15 mm	N.A.	N.A.

3. Methods

3.1. The CIE Color Values and Delta E (ΔE)

Color measurements were conducted using an X-Rite spectrophotometer, which operates within a spectral range of 380–780 nm, utilizes a D50 filter, and features a 2° measurement geometry and a 4.5 mm aperture diameter. The L*a*b* color values of the printed materials were measured, and their Total Color Difference (ΔE) was assessed in comparison to the benchmark values specified by the ISO 12647-5 (2015) [48] standard for screen printing. The 12647 series prepared by ISO generally concerns printing processes' standardization and quality control. The ISO 12647-5 (2015) standard is specifically related to screen printing.

In the L*a*b* color space, L* signifies lightness, extending from 100 (denoting white) to 0 (representing black). Concurrently, the a* and b* components articulate chromaticity, defined as the attribute of a color distinct from its luminance. Notably, a* and b* represent color orientations: –a* aligns with the green axis and +a* with the red axis, whereas –b* corresponds to the blue axis and +b* to the yellow for the stone paper axis [49].

ΔE reveals the difference between the displayed and original colors [50]. Specifically, the ΔE_{00} formula includes special terms that enhance the performance of interactions between color tones, particularly improving the performance of blue and gray colors [51]. Lower ΔE values indicate high accuracy between the colors, while higher ΔE values indicate an inconsistency between the colors. ΔE values range between 0 and 100; values of < 1 indicate a color difference that cannot be perceived by the human eye, between 1 and 2 indicate a color difference that can be perceived upon close observation; between 2 and 10 indicate an acceptable color difference at a glance, between 11 and 49 indicate a significant color difference, and a value of 100 indicates opposite colors. Keeping constant the CIE L*a*b* color values, the color difference value (ΔE_{00}) of other inks was calculated using Equation (1).

$$\Delta E_{00} = \sqrt{\left(\frac{\Delta L'}{k_L S_L}\right)^2 + \left(\frac{\Delta C'}{K_C S_C}\right)^2 + \left(\frac{\Delta H'}{K_H S_H}\right)^2 + R_T\left(\frac{\Delta C'}{K_C S_C}\right)\left(\frac{\Delta H'}{K_H S_H}\right)} \quad (1)$$

where R_T is the hue rotation term, K_L, K_C, and K_H are parametric factors, L, C, and H represent compensation for neutral colors, S_L is compensation for lightness, S_C is compensation for chroma, and S_H is compensation for hue [22,52–54].

In the ISO 12647-5 (2015) standard for screen printing, three distinct color gamuts for CMYK (cyan, magenta, yellow, and black) ink sets are specified as small, medium, and large. The large gamut L*a*b* references indicate more saturated color values than small and medium gamuts within the same standard. For instance, the medium gamut cyan color value in ISO 12647-5 (2015) is provided as L: 52, a: −33, b: −51, and the large gamut cyan color value is L: 46, a: −32, b: −54, demonstrating the higher saturation of the large gamut [49,55].

3.2. Lightfastness Tests

The lightfastness of a color is a measure of its resistance to fading under sunlight. The color fastness of pigments is of fundamental importance for the lightfastness of printing inks and their resistance to weather conditions, color quality, and durability [56,57]. Colorants

can be divided into broad lightfastness classes and determined based on the blue wool scale. In general, the lightfastness of a pigment decreases with the degree to which it is diluted by other pigments, mainly white pigments. Highly concentrated color inks have better light resistance due to the self-masking effect of the pigments [24].

Lightfastness tests were conducted using a Xenotest 150 S+ device and the blue wool scale according to the conditions specified in the ISO 12040:1997 [58] standard. The blue wool scale was measured using the DIN EN ISO 105-A02 [59] standard. The L*a*b* values of the test printing samples were measured every 24 h before and after the lightfastness tests, and ΔE values were calculated and compared. Lightfastness tests were conducted on five different samples for each paper type. The color fading of each sample was measured three times.

3.3. Ink Consumption

To measure the ink consumption of two different test printed papers, five samples for each mesh count were weighed with a Mettler Toledo AB304-S before and after the printing and drying processes. Each sample was measured three times, and their arithmetic average was taken to determine ink consumption.

3.4. Printing Machine and Conditions

Test prints were conducted in a laboratory environment at 23 °C and 65% relative humidity using an Arus-brand semi-automatic screen printing machine equipped with a 2 mm snap-off. The purpose of selecting this machine was to ensure constant printing conditions (e.g., squeegee angle, squeegee pressure) for each print. This will ensure the same ink consumption for each repeated sample printing.

The papers intended for printing were brought to the test printing laboratory 24 h in advance. For each type of paper and mesh count, five prints were produced. Following the printing process, samples using solvent-based inks were allowed to dry in the laboratory for 24 h, while those using UV-based inks were dried using a Super Primex EB-200 pm dryer.

3.5. Surface Contact Angle

The surface contact angle is a parameter used to determine the resistance of a paper surface to liquids. The resultant data are used to determine the printing quality. The surface wetting capacity of the ink designates the printing efficiency [60,61]. The contact angle indicates the degree of wetness. A contact angle of 0° indicates maximum wetting, a contact angle between 0 and 90° indicates partial wetting, and an angle of >90° indicates no wetting [62]. The contact angle was measured with a contact angle meter (Attension, Theta Lite 101) by placing a droplet of 5 µL of deionized water onto the surface of the specimens. Measurements were taken from five different samples of each of the two paper types, and the average value results were taken. And each sample was measured three times.

3.6. Scanning Electron Microscopy (SEM) Measurements

SEM measurements were carried out in an EDS (Bruker) device (brand: ZEISS, model: EVO LS10, detectors: SE, BSD, STEM, Carl Zeiss Microscopy GmbH, Berlin, Germany). Images were captured using a Secondary Electron (SE) detector, and a gold coating was applied for conductivity. Images of the printed stone paper and coated sticker paper were recorded on the SEM device. Images of solvent-ink-printed samples were taken at 100-, 500-, and 1000-times magnification. Both the unprinted paper surfaces and the ink behavior on these surfaces were examined and compared in these images.

3.7. Rub Resistance

Ink scuffing or rubbing resistance refers to the degree to which the ink layer is scratched and peeled off under the action of scuffing. Primary factors affecting this resistance are the basic properties of the paper (smoothness, absorbency, etc.), the ink composition, and

the printing conditions. Differences in printing density can lead to color changes, so color differences can also describe the rubbing resistance [63].

A TMI-brand Ink Rub Tester was used to measure the rubbing resistance of the printed samples. Tests were performed according to the TAPPI T-830 [64] standard. In the present experiment, wear on the inked layers was induced by rubbing the printed surfaces against the same type of unprinted paper layers. In accordance with the TAPPI T-830 standard, a constant rubbing pressure was applied to the printed and unprinted samples using a 907 gr (2 lb) weight. For each sample, rubbing was set to 50 cycles, and density and L*a*b* measurements were carried out for every 50 rubbings. A total of 300 rubbings were performed for each sample. In the rub resistance tests, measurements were conducted on five different printed samples for each paper type and mesh count. Each sample was measured three times, and their arithmetic averages were calculated. The rub resistance of the prints was calculated using Equation (2) [65].

$$\text{Rub resistance index (RI)} = \frac{\text{Density after rub}}{\text{Density before rub}} \times 100 \quad (2)$$

4. Results and Discussions

4.1. Lightfastness

In the lightfastness tests, two different ink types were printed on both substrates, and fading was observed. The blue wool test scale used in the lightfastness tests after 168 h of fading and the samples used in the experiment are presented in Figures 2 and 3.

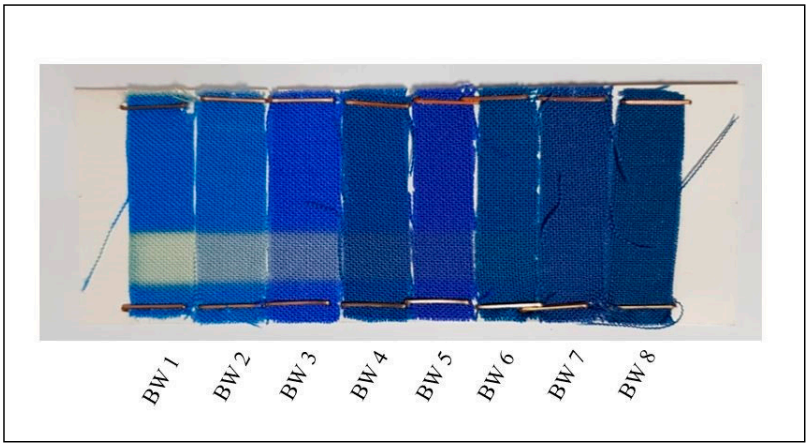

Figure 2. The blue wool scale test used in lightfastness tests after 168 h of fading.

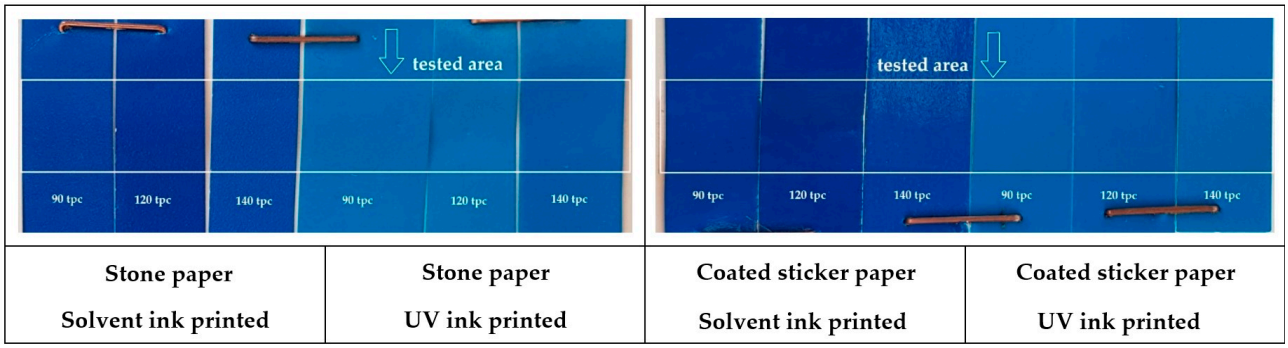

Figure 3. Appearance of test printed papers after 168 h of lightfastness tests.

The samples printed with each mesh count were subjected to the lightfastness test under the same conditions (Figure 3).

As a result of fading (168 h), which corresponds to five-fourths in the blue wool scale, the maximum ΔE value did not exceed 1.36 for the solvent ink and 1.29 for the UV-based

ink. Both values were below the CIELAB (CIE L*a*b*) ΔE limits for cyan ink in ISO 12647-5 (2015). The before and after lightfastness values can be seen in Tables 2 and 3 (SE: the standard error value has been added next to each measurement). As can be seen in Table 3, the UV ink had higher lightfastness than the solvent-based ink on stone paper. In general, the ΔE on the stone paper was higher than on the coated sticker paper since stone paper is not absorbent and the ink dried on the surface, whereas coated sticker paper has a fibrous texture and absorbs ink. So, the light used in the lightfastness test had limited penetration into the fibers.

Table 2. Density and L*a*b* measurements before lightfastness test with standard error (SE) values.

Mesh Count	Ink Type	Stone Paper								Coated Sticker Paper							
		Density	SE	L*	SE	a*	SE	b*	SE	Density	SE	L*	SE	a*	SE	b*	SE
90 tpc	Solvent	2.76	0.01	30.41	0.07	−7.57	0.04	−60.01	0.06	2.83	0.01	27.90	0.05	−6.02	0.02	−58.38	0.02
120 tpc	Solvent	2.62	0.01	33.93	0.02	−12.96	0.03	−59.87	0.03	2.81	0.00	32.98	0.05	−13.31	0.03	−58.88	0.02
140 tpc	Solvent	2.60	0.02	35.11	0.01	−13.86	0.04	−59.76	0.03	2.80	0.00	34.32	0.02	−14.60	0.02	−59.55	0.02
90 tpc	UV	2.24	0.01	43.58	0.03	−24.84	0.05	−54.55	0.04	2.06	0.01	44.09	0.03	−21.82	0.03	−51.48	0.02
120 tpc	UV	1.88	0.02	47.29	0.06	−28.88	0.02	−52.20	0.05	1.93	0.01	46.04	0.03	−24.38	0.02	−50.89	0.01
140 tpc	UV	1.79	0.00	48.32	0.03	−29.30	0.05	−51.55	0.02	1.85	0.00	47.45	0.03	−25.43	0.04	−49.78	0.02

Table 3. ΔE_{00} values of stone paper and coated sticker paper after lightfastness test.

Mesh Count	Ink Type	Stone Paper							Coated Sticker Paper						
		L*	SE	a*	SE	b*	SE	ΔE_{00}	L*	SE	a*	SE	b*	SE	ΔE_{00}
90 tpc	Solvent	29.97	0.02	−5.39	0.02	−59.47	0.03	1.36	29.00	0.02	−5.83	0.01	−59.58	0.03	0.86
120 tpc	Solvent	33.36	0.00	−10.91	0.01	−59.33	0.02	1.21	32.53	0.01	−11.33	0.01	−59.86	0.02	1,03
140 tpc	Solvent	36.24	0.01	−14.02	0.02	−58.94	0.02	0.95	34.26	0.02	−13.37	0.02	−60.14	0.02	0.60
90 tpc	UV	43.57	0.03	−24.51	0.03	−56.36	0.03	0.52	44.52	0.03	−22.67	0.02	−50.25	0.03	0.68
120 tpc	UV	46.63	0.02	−27.01	0.02	−54.42	0.01	1.29	45.60	0.01	−24.23	0.02	−49.87	0.01	0.50
140 tpc	UV	48.07	0.01	−27.99	0.02	−52.94	0.02	0.80	47.41	0.02	−26.33	0.02	−47.84	0.02	0.77

4.2. Absorbance and Ink Consumption

In the contact angle measurements, the water spread was greater on the coated sticker paper. These results showed that the coated sticker paper had a more absorbent texture than the stone paper (Figure 4).

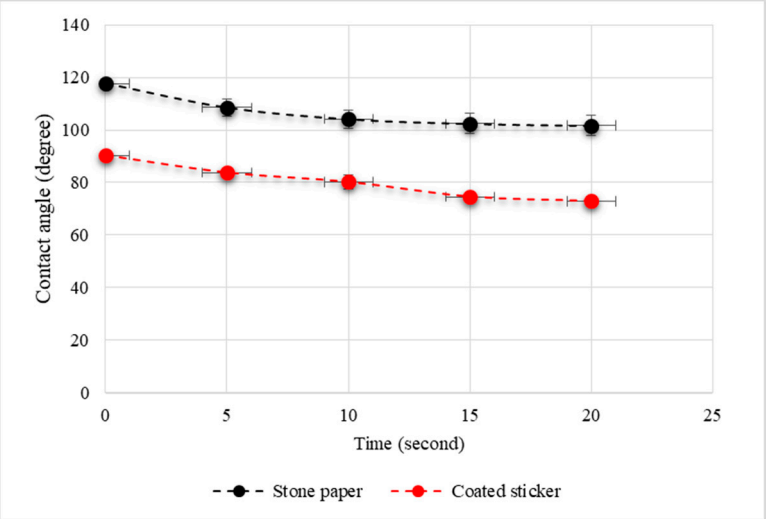

Figure 4. Time-dependent changes in surface contact angles for unprinted papers.

By measuring the mass of each paper before and after printing, the amount of ink consumed by these papers was determined. The ink consumption measurements revealed that the density values and ink consumption were greater on the coated sticker paper than on the stone paper. The density values of all the solvent ink prints were higher than those

of the UV-based ink prints (Table 4). Especially in the prints made with solvent-based inks, the ink consumption on the coated sticker paper was twice as much as on the stone paper (Table 5).

Table 4. Density measurements of papers.

Mesh Count	Ink Type	Stone Paper		Coated Sticker Paper	
		Density	SE	Density	SE
90 tpc	Solvent	2.76	0.01	2.83	0.01
120 tpc	Solvent	2.62	0.01	2.81	0.00
140 tpc	Solvent	2.60	0.02	2.80	0.00
90 tpc	UV	2.24	0.01	2.06	0.01
120 tpc	UV	1.88	0.02	1.93	0.01
140 tpc	UV	1.79	0.00	1.85	0.00

Table 5. Ink consumption measurements.

Mesh Count	Solvent-Based Ink				UV-Based Ink			
	Stone Paper		Coated Sticker Paper		Stone Paper		Coated Sticker Paper	
Unit	g/m^2	SE	g/m^2	SE	g/m^2	SE	g/m^2	SE
90 tpc	8.06	0.04	15.53	0.02	18.18	0.03	26.68	0.03
120 tpc	6.35	0.03	14.96	0.03	16.92	0.03	23.76	0.02
140 tpc	5.86	0.05	13.92	0.04	14.38	0.02	23.01	0.02

As the surface contact angle increases, the ink consumption decreases (Figure 4 and Table 5). Stone paper has a non-absorbent polymer surface; thus, a higher surface contact angle was measured than for the coated sticker paper (Figure 4). This reduces the absorbency of stone paper, causing ink consumption to remain low. Coated sticker paper, on the other hand, has an absorbent cellulosic surface, thus allowing the surface contact angle to decrease. The absorbent cellulosic structure of coated sticker paper is also an essential factor in the high ink consumption of coated sticker paper.

4.3. Surface Contact Angle

The changes in the surface contact angles of the stone paper and the coated sticker paper over time are presented in Figure 4. Both materials' surface contact angles were measured at the dripping moment and every five seconds after that. For the stone paper, the surface contact angle was 117.6° at the time of the first drop, 108.5° by the 5th second, 104.1° by the 10th second, 102.4° by the 15th second, and 101.7° by the 20th second. For the coated sticker paper, the surface contact angle was 90.3° at the time of the first drop, 83.7° by the 5th second, 80.2° by the 10th second, 74.6° by the 15th second, and 72.9° by the 20th second. At the end of the 20 s average measurement period, the surface contact angle was 106.9° for the stone paper and 80.3° for the coated sticker paper.

Coated sticker paper absorbs and spreads water drops due to its cellulosic structure. Thus, its surface contact angle decreases. Due to the polymer structure of stone paper, it is hydrophobic, resulting in a high surface contact angle (Figure 4).

4.4. SEM Images

SEM images of samples printed with solvent ink with a 120 tpc mesh count are presented in Figure 5. Images a, b, and c in Figure 5 were taken at 100-, 500-, and 1000-times magnification, respectively. In Figure 5a, indentations and protrusions can be seen along the line in the middle area where the ink prints end on the stone paper. In Figure 5b, since the image is enlarged 500 times, the indented areas in the middle region of the stone paper are more visible, and the rough surface in the unprinted region of the same image is more noticeable. In contrast, a smoother line is seen in the middle region where the

printed surface on the coated sticker paper surface lies in Figure 5b. Finally, in Figure 5c, with 1000 times magnification, the smooth structure of the coated sticker paper and the ink printed on it without smearing can be seen more clearly, while the distinct rough surface of the stone paper and the distribution of the ink on this rough surface can be seen more clearly.

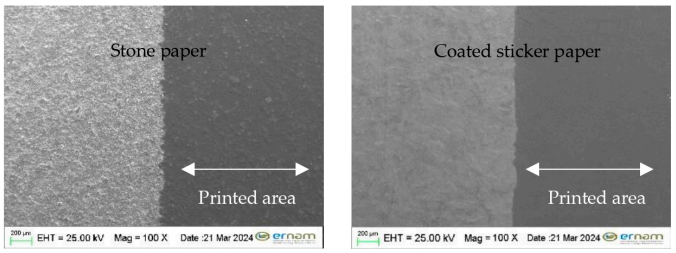

a) 100 times enlargement

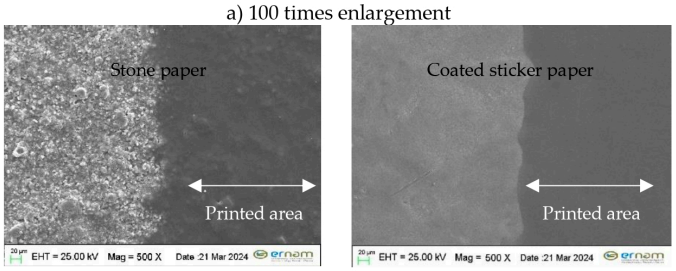

b) 500 times enlargement

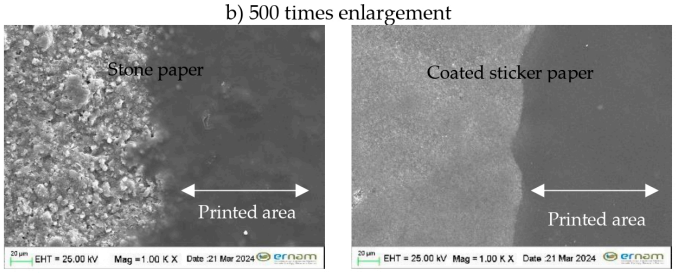

c) 1000 times enlargement

Figure 5. SEM images of papers printed with solvent ink and a 120 tpc screen (EHT: Extra High Tension, Mag: Magnification).

Images were taken of the complete ink-printed surfaces of both papers to better see the ink behavior on the coated sticker paper and stone paper on the printed surface (Figure 6). As explained in the previous figure (Figure 5), the smooth surface of the coated sticker paper gave rise to a smoother ink-printed surface than the stone paper. The surface of the stone paper also had a rough appearance after ink printing. The print densities of both samples were close to each other (coated sticker paper print density: 2.8 and stone paper print density: 2.65).

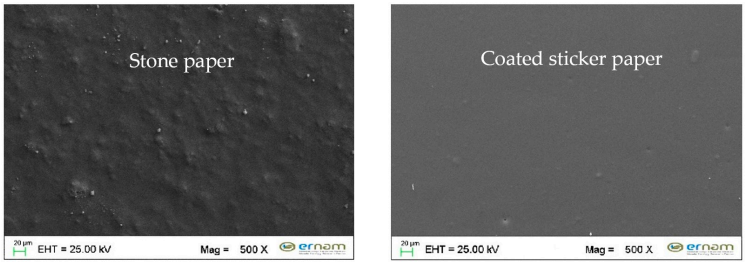

Figure 6. SEM images at 500-times enlargement of solvent-ink-printed papers with a 120 tpc screen. Both surfaces are fully printed.

4.5. Rub Resistance

The rubbing resistance of UV-based ink was relatively high on both papers. Only the adhesion on the coated sticker paper was slightly higher (between 99.26 and 99.82%). Such a case can be attributed to the cellulosic structure of coated sticker paper and the good absorption of liquid UV ink. The polymerization of UV-based ink during drying played a significant role in the high rubbing resistance of both paper types (97–99%) (Table 6) [66,67]. For the rubbing resistance of solvent ink, adhesion on the stone paper was higher than that on the coated sticker paper (between 86.98 and 90.05%). Solvent ink accumulated on the non-absorbent surface of the stone paper and dried as a resistant layer (Table 6).

Table 6. Stone paper and coated sticker paper rubbing resistance.

Mesh Count	Ink Type	Stone Paper					Coated Sticker Paper				
		Printing Density before Rubbing Test		Printing Density after Rubbing Test		Percentage Retained after Rubbing Test	Printing Density before Rubbing Test		Printing Density after Rubbing Test		Percentage Retained after Rubbing Test
		Density	SE	Density	SE	%	Density	SE	Density	SE	%
90 tpc	solvent	2.69	0.02	2.34	0.03	86.98	2.81	0.01	2.16	0.05	76.75
120 tpc	solvent	2.65	0.01	2.31	0.02	87.40	2.80	0.01	2.48	0.03	88.80
140 tpc	solvent	2.61	0.01	2.35	0.02	90.05	2.71	0.02	1.78	0.07	65.60
90 tpc	UV	2.27	0.00	2.23	0.01	97.94	2.06	0.01	2.05	0.01	99.51
120 tpc	UV	1.91	0.01	1.90	0.01	99.47	1.95	0.01	1.94	0.01	99.82
140 tpc	UV	1.79	0.01	1.78	0.01	99.07	1.81	0.00	1.80	0.01	99.26

The printing density of the coated sticker paper was generally higher than that of the stone paper. The UV-based-ink-printed surfaces exhibited stable rubbing resistance on both papers (Figure 7, Table 6).

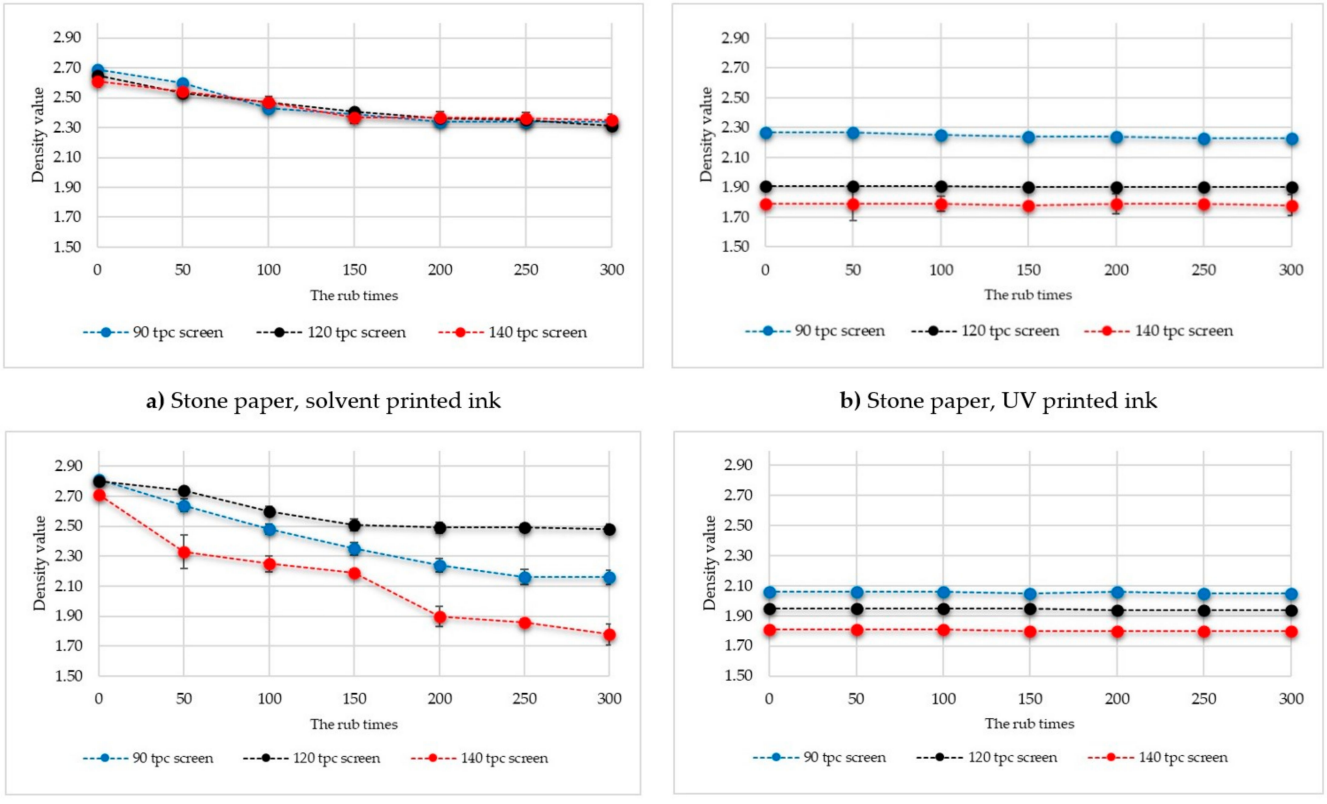

a) Stone paper, solvent printed ink

b) Stone paper, UV printed ink

c) Coated sticker paper, solvent printed ink

d) Coated sticker paper, UV printed ink

Figure 7. Ink rubbing resistances on stone paper and coated sticker paper.

In Figure 7a, the solvent ink layers printed with three different mesh counts on the stone paper showed regular abrasion with the number of rubs. However, as can be seen in Figure 7b, the UV ink layers printed with the same mesh count on the same paper layer showed high rub resistance. This resistance can be explained by the polymerization and curing of the UV ink, which form a stable surface. A similar observation was made on the coated sticker paper; as shown in Figure 7c, wear increased parallel to the number of rubs in the printing of the solvent ink on the coated sticker paper. In contrast, the rub resistance of the UV ink printed on the coated sticker paper was found to be quite high (Figure 7d).

When evaluating the rub resistance of solvent inks independently, a consistent decrease is observed in Figure 7c. This reduction can be attributed to the fact that solvent-based inks undergo physical drying through evaporation and do not form a polymeric structure. Such drying does not provide as stable a structure as UV-cured inks. In UV curing, a photopolymerization process is utilized. Consequently, this process leads to rapid polymerization, which facilitates the swift drying of the ink film and provides a more stable film layer compared to solvent-based inks [24,30].

The color changes in the substrates printed with solvent ink are shown by the ΔE values before and after the rub resistance tests, as provided in Table 7. Due to the absorptive nature of coated paper, the solvent ink was absorbed into these surfaces and did not form as strong a bond as on the stone paper. This situation is also evident in the abrasion values listed in Table 6. This abrasion is more pronounced in the ΔE values of the ink printed on the coated paper with a 140 tpc mesh (where the density value is the lowest), as shown in Table 7.

Table 7. ΔE values after rubbing resistance test of solvent-ink-printed substrates.

Mesh Count	Material	Ink Type	Printing L*a*b* before Rubbing Test						Printing L*a*b* after Rubbing Test						ΔE_{00}
			L*	SE	a*	SE	b*	SE	L*	SE	a*	SE	b*	SE	
90 tpc	Stone paper	solvent	29.93	0.08	−6.65	0.21	−59.86	0.15	33.17	0.19	−7.30	0.16	−57.08	0.23	2.60
120 tpc	Stone paper	solvent	33.16	0.14	−11.46	0.17	−59.84	0.06	35.03	0.17	−11.10	0.21	−57.83	0.15	1.61
140 tpc	Stone paper	solvent	35.50	0.19	−14.36	0.22	−60.30	0.04	36.45	0.24	−13.46	0.13	−58.52	0.20	1.04
90 tpc	Coated sticker paper	solvent	28.21	0.13	−6.18	0.18	−58.72	0.05	30.53	0.10	−6.17	0.24	−55.55	0.21	1.93
120 tpc	Coated sticker paper	solvent	32.46	0.17	−12.35	0.12	−59.22	0.05	33.52	0.21	−12.91	0.41	−57.80	0.13	0.92
140 tpc	Coated sticker paper	solvent	34.43	0.03	−14.47	0.04	−59.63	0.06	38.66	0.64	−12.19	0.50	−54.11	0.69	4.05

As explained above, it can be seen more clearly in the graphs below that UV-based inks (Figure 7b,d) have higher friction resistance than solvent-based inks (Figure 7a,c).

5. Conclusions

For the stone paper printed with UV-based ink, a 120 tpc screen yielded close values to the large gamut specified in the ISO 12647-5 (2015) standard. Users using the large gamut as a reference can print with a mesh count of 120 tpc.

In the present experiments, screens with three different mesh counts were used, and three ink layers with differing optical densities were printed. The lightfastness of each different ink layer was high. Based on the present findings, printing with a 140 tpc screen can be recommended since an ink layer with high lightfastness can be printed with less ink consumption.

The rubbing tests revealed that the UV-based inks had high rubbing resistance values at every mesh count. Moreover, since we measured that ink consumption decreases with increasing the mesh count, we can say that ink savings will be achieved by using more frequent meshes.

Considering ink consumption, especially when printing with solvent ink, the ink consumption of the coated sticker paper was approximately twice as high as that of the stone paper. On the other hand, the optical ink density ratios of both papers were measured as being close to each other. Savings in ink consumption, thus cost savings, will be achieved when printing with stone paper.

Currently, the consumption of natural resources is increasing rapidly. Plants and forests, which are sources of cellulose products, have many benefits for the environment, including climate regulation, biodiversity protection, oxygen production, and erosion prevention. Besides sustainable forest management and nature protection, the potential use of stone paper in the printing industry as an alternative to cellulose-based papers will also offer an essential option for a sustainable environment.

Screen printing is frequently used in outdoor printing, thanks to its advantages. Stone paper may be considered instead of petroleum resin printing materials used outdoors. Stone paper, which has high water and oil resistance, can be considered an alternative for outdoor printing and other areas that require durable printing substrates.

Author Contributions: Methodology, C.A.; Investigation, C.A.; Resources, C.A.; Writing—review & editing, C.A. and A.A.; Supervision, A.A. All authors have read and agreed to the published version of the manuscript.

Funding: This research received no external funding.

Institutional Review Board Statement: Not applicable.

Informed Consent Statement: Not applicable.

Data Availability Statement: The raw data supporting the conclusions of this article will be made available by the authors on request.

Conflicts of Interest: The authors declare no conflicts of interest.

References

1. *Handbook of Print Media*; Europe Print Papers: Uppsala, Sweden, 2001; Volume 13, p. 35.
2. Banks, C.E.; Foster, C.W.; Kadara, R.O. *Screen-Printing Electrochemical Architectures*; SpringerBriefs in Applied Sciences and Technology; Springer International Publishing: Cham, Switzerland, 2016; ISBN 978-3-319-25191-2.
3. Lee, T.M.; Choi, Y.J.; Nam, S.Y.; You, C.W.; Na, D.Y.; Choi, H.C.; Shin, D.Y.; Kim, K.Y.; Jung, K.I. Color Filter Patterned by Screen Printing. *Thin Solid Films* **2008**, *516*, 7875–7880. [CrossRef]
4. Boda, U.; Petsagkourakis, I.; Beni, V.; Andersson Ersman, P.; Tybrandt, K. Fully Screen-Printed Stretchable Organic Electrochemical Transistors. *Adv. Mater. Technol.* **2023**, *8*, 2300247. [CrossRef]
5. Khan, S.; Lorenzelli, L.; Dahiya, R.S. Technologies for Printing Sensors and Electronics over Large Flexible Substrates: A Review. *IEEE Sens. J.* **2015**, *15*, 3164–3185. [CrossRef]
6. Indriati, L.; Nugraha, M.A.; Perng, Y.S. Stone Paper, an Eco-Friendly and Free-Tree Papers. *AIP Conf. Proc.* **2020**, *2243*, 030010.
7. Teed, L.; Bélanger, D.; Gagnon, P.; Edinger, E. Calcium Carbonate ($CaCO_3$) Production of a Subpolar Rhodolith Bed: Methods of Estimation, Effect of Bioturbators, and Global Comparisons. *Estuar. Coast. Shelf Sci.* **2020**, *242*, 106822. [CrossRef]
8. Chave, K.E.; Smith, S.V.; Roy, K.J. Carbonate Production by Coral Reefs. *Mar. Geol.* **1972**, *12*, 123–140. [CrossRef]
9. Anbu, P.; Kang, C.H.; Shin, Y.J.; So, J.S. Formations of Calcium Carbonate Minerals by Bacteria and Its Multiple Applications. *Springerplus* **2016**, *5*, 250. [CrossRef]
10. Stocks-Fischer, S.; Galinat, J.K.; Bang, S.S. Microbiological Precipitation of $CaCO_3$. *Soil Biol. Biochem.* **1999**, *31*, 1563–1571. [CrossRef]
11. Swain, N.; Saini, P.; Bhati, S.S.; Rastogi, V.K. Biodegradable Stone Paper as a Sustainable Alternative to Traditional Paper: A Review. *J. Inorg. Organomet. Polym. Mater.* **2023**, *33*, 2240–2251. [CrossRef]
12. Thunwall, M.; Kuthanová, V.; Boldizar, A.; Rigdahl, M. Film Blowing of Thermoplastic Starch. *Carbohydr. Polym.* **2008**, *71*, 583–590. [CrossRef]
13. Dziadowiec, D.; Matykiewicz, D.; Szostak, M.; Andrzejewski, J. Overview of the Cast Polyolefin Film Extrusion Technology for Multi-Layer Packaging Applications. *Materials* **2023**, *16*, 1071. [CrossRef] [PubMed]
14. Khare, R.; Khare, S. Polymer and Its Effect on Environment. *J. Indian Chem. Soc.* **2023**, *100*, 100821. [CrossRef]
15. Krasowska, K.; Heimowska, A. Degradability of Polylactide in Natural Aqueous Environments. *Water* **2023**, *15*, 81–87. [CrossRef]
16. Gironi, F.; Piemonte, V. Bioplastics and Petroleum-Based Plastics: Strengths and Weaknesses. *Energy Sources Part A Recover. Util. Environ. Eff.* **2011**, *33*, 1949–1959. [CrossRef]

17. Pang, M. Completely Biodegradable Stone Paper Material and Preparation Method Thereof. 2015. Available online: https://patents.google.com/patent/CN103131145B/en (accessed on 26 March 2024).
18. Varodi, C.; Pogacean, F.; Gheorghe, M.; Mirel, V.; Coros, M.; Barbu-Tudoran, L.; van Staden, R.I.S.; Pruneanu, S. Stone Paper as a New Substrate to Fabricate Flexible Screen-Printed Electrodes for the Electrochemical Detection of Dopamine. *Sensors* **2020**, *20*, 3609. [CrossRef]
19. Truman, A.B.; Munday, F.D. The Printability of Synthetic and Plastics Paper. In *The Fundamental Properties of Paper Related to its Uses*; FRC: Manchester, UK, 1973; pp. 573–599. [CrossRef]
20. Hsieh, Y.C.; Lee, K.K.; Cheng, S.Y.; Kao, C.C. Offset Printing Quality Characteristics of Rich Mineral Paper. *Appl. Mech. Mater.* **2013**, *262*, 320–323. [CrossRef]
21. Chu, C.; Nel, P. Characterisation and Deterioration of Stone Papers. *AICCM Bull.* **2019**, *40*, 37–49. [CrossRef]
22. Yüce, H.; Genç, G.; Sönmez, S.; Özden, Ö.; Akgül, A.; Çetiner, B.N. Printability of Bio-Composite Sheets Made from Paper Mill and Cardboard Mill Waste Sludge. *Pigment Resin Technol.* **2022**, *51*, 541–549. [CrossRef]
23. Sonmez, S.; Genc, G.; Yuce, H. How Does the Surface Topography of a Green Composite Affect Its Printability? *J. Eng. Appl. Sci.* **2019**, *2*, 55–60.
24. Leach, R.H.; Pierce, R.J.; Hickman, E.P.; Mackenzie, M.J.; Smith, H.G. (Eds.) *The Printing Ink Manual*; Springer: Dordrecht, The Netherlands, 1993; ISBN 978-0-948905-81-0.
25. Hyun, W.J.; Secor, E.B.; Hersam, M.C.; Frisbie, C.D.; Francis, L.F. High-Resolution Patterning of Graphene by Screen Printing with a Silicon Stencil for Highly Flexible Printed Electronics. *Adv. Mater.* **2015**, *27*, 109–115. [CrossRef]
26. Kobs, D.R.; Voigt, D.R. Parametric Dependencies in Thick-Film Screening. *Microelectron. Reliab.* **1971**, *10*, 311–312. [CrossRef]
27. Jewell, E.H.; Claypole, T.C.; Gethin, D.T. The Influence of Squeegee Parameters on Ink Deposit in UV Halftone Screen Printing. *TAGA J.* **2006**, *3*, cronfa37706.
28. Ali, M.; Lin, L.; Faisal, S.; Sahito, I.A.; Ali, S.I. Optimisation of Screen Printing Process for Functional Printing. *Pigment Resin Technol.* **2019**, *48*, 456–463. [CrossRef]
29. Novaković, D.; Kašiković, N.; Vladić, G.; Pál, M. *Screen Printing*; William Andrew Publishing: Norwich, NY, USA, 2015; pp. 247–261. [CrossRef]
30. Özdemir, L.; Kurt, M.B.; Akgül, A.; Oktav, M.; Nayci Duman, M. Optimization of Ink Consumption in Screen Printing within Color Difference Limits. *Pigment Resin Technol.* **2022**, *53*, 17–27. [CrossRef]
31. Stančić, M.; Novaković, D.; Tomić, I.; Karlović, I. Influence of Substrate and Screen Thread Count on Reproduction of Image Elements in Screen Printing. *Acta Graph.* **2012**, *23*, 1–12.
32. Pan, J.; Tonkay, G.L.; Storer, R.H.; Sallade, R.M.; Leandri, D.J. Critical Variables of Solder Paste Stencil Printing for Micro-BGA and Fine-Pitch QFP. *IEEE Trans. Electron. Packag. Manuf.* **2004**, *27*, 125–132. [CrossRef]
33. Wang, J. Electrochemical Glucose Biosensors. In *Electrochemical Sensors, Biosensors and their Biomedical Applications*; Academic Press: New York, NY, USA, 2008; pp. 57–69. [CrossRef]
34. Liu, M.; Zhang, Q.; Zhao, Y.; Shao, Y.; Zhang, D. Design and Development of a Fully Printed Accelerometer with a Carbon Paste-Based Strain Gauge. *Sensors* **2020**, *20*, 3395. [CrossRef]
35. Barkhouse, D.A.R.; Gunawan, O.; Gokmen, T.; Todorov, T.K.; Mitzi, D.B. Yield Predictions for Photovoltaic Power Plants: Empirical Validation, Recent Advances and Remaining Uncertainties. *Prog. Photovolt. Res. Appl.* **2015**, *20*, 6–11. [CrossRef]
36. Van Duppen, J. *Manual for Screen Printing*; Verlag Der Siebdruck: Lübeck, Germany, 1987; ISBN 3925402217.
37. *SCNS 1352*; Method of Test for Grammage of Paper and Board. Chinese National Standards: Taipei, Taiwan, 2012.
38. *CNS 3685*; Method of test for thickness and apparent density of paper and board. Chinese National Standards: Taipei, Taiwan, 2018.
39. *CNS 12885*; Pulp Cement Perlite Boards. Chinese National Standards: Taipei, Taiwan, 2017.
40. *CNS 14931*; Paper and paperboard—Determination of opacity (paper backing)—Diffuse reflectance method. Chinese National Standards: Taipei, Taiwan, 2018.
41. *GB 13022-91*; Plastics-Determination of tensile properties of films. Standardization Administration of China: Beijing, China, 1991.
42. *GBT 12027-2004*; Plastics—Film and sheeting—Determination of dimensional change on heating. Standardization Administration of China: Beijing, China, 2004.
43. *QB/T 1130-91*; Plastics Angle Tear Performance Test Method. Ministry of Light Industry of the People's Republic of China: Beijing, China, 1991.
44. *ISO 536*; Paper and Board—Determination of Grammage. International Organization for Standardization (ISO): Geneva, Switzerland, 2019.
45. *ISO 534*; Paper and board—Determination of thickness, density and specific volume. International Organization for Standardization (ISO): Geneva, Switzerland, 2011.
46. *ISO 2470-2*; Paper, Board and Pulp—Measurement of Diffuse Blue Reflectance Factor—Part 2: Outdoor Daylight Conditions (D65 Brightness). International Organization for Standardization (ISO): Geneva, Switzerland, 2008.
47. *ISO 1924-3*; Paper and Board—Determination of Tensile Properties—Part 3: Constant Rate of Elongation Method (100 mm/min). International Organization for Standardization (ISO): Geneva, Switzerland, 2005.
48. *ISO 12647-5*; Graphic technology—Process control for the production of half-tone colour separations, proof and production prints—Part 5: Screen printing. International Organization for Standardization (ISO): Geneva, Switzerland, 2015.

49. Belasco, R.; Edwards, T.; Munoz, A.J.; Rayo, V.; Buono, M.J. The Effect of Hydration on Urine Color Objectively Evaluated in CIE L*a*b* Color Space. *Front. Nutr.* **2020**, *7*, 576974. [CrossRef]
50. Petersson, J. A Review of Perceptual Image Quality. Linköpings Universitet: Linköpings, Sweden, 2005.
51. Luo, M.R.; Cui, G.; Rigg, B. The Development of the CIE 2000 Colour-Difference Formula: CIEDE2000. *Color Res. Appl.* **2001**, *26*, 340–350. [CrossRef]
52. Blaznik, B.; Možina, K.; Bračko, S. Stability of Ink-Jet Prints under Influence of Light. *Nord. Pulp Pap. Res. J.* **2013**, *28*, 111–118. [CrossRef]
53. Debeljak, M.; Bračko, S.; Hladnik, A.; Gregor-Svetec, D. Comparison of Ultraviolet Inkjet Printing on Different Synthetic Fibrous Papers. *Tappi J.* **2010**, *9*, 17–25. [CrossRef]
54. Sönmez, S.; Arslan, S. Investigation of the Effects on Ink Colour of Lacquer Coating Applied to the Printed Substrate in the Electrophotographic Printing System. *Pol. J. Chem. Technol.* **2021**, *23*, 35–40. [CrossRef]
55. Schwiegerling, J. *Field Guide to Visual and Ophthalmic Optics*; Spie: Bellingham, WA, USA, 2004; ISBN 9780819456298.
56. Aydemir, C.; Yenidoğan, S. Light Fastness of Printing Inks: A Review. *J. Graph. Eng. Des.* **2018**, *9*, 37–43. [CrossRef]
57. Özomay, Z.; Söz, Ç.K.; Sönmez, S. Investigation of the Effect of Light Fastness on the Color Changes of Maps Prepared by Electrophotographic Digital Printing. *Nord. Pulp Pap. Res. J.* **2022**, *37*, 184–191. [CrossRef]
58. *ISO 12040:1997*; Graphic technology—Prints and printing inks—Assessment of light fastness using filtered xenon arc light. International Organization for Standardization (ISO): Geneva, Switzerland, 1997.
59. *DIN EN ISO 105-A02*; Textiles—Tests for colour fastness—Part A02: Grey scale for assessing change in colour. Deutsches Institut für Normung (DIN): Berlin, Germany, 1993.
60. Etzler, F.M.; Conners, J.J. The Surface Chemistry of Paper: Its Relationship to Printability and Other Paper Technologies. In *Surface Analysis of Paper*; CRC Press: Boca Raton, FL, USA, 2020; pp. 90–108.
61. Sonmez, S.; Sood, S.; Li, K.; Salam, A.; Fleming, P.D.; Pekarovicova, A.; Wu, Q. Effect of Progressive Deinking and Reprinting on Inkjet-Printed Paper. *Nord. Pulp Pap. Res. J.* **2023**, *38*, 131–140. [CrossRef]
62. Salapare, H.S.; Blantocas, G.Q.; Noguera, V.R.; Ramos, H.J. The Porosity And Wettability Properties Of Hydrogen Ion Treated Poly(Tetrafluoroethylene). *Contact Angle Wettability Adhes.* **2009**, *6*, 207–216. [CrossRef]
63. Zhou, W.H.; He, B.H.; Zhang, C.X.; Han, Y. Analysis on Ink Layer Rub Resistance for Coated Paper Prints. *Adv. Mater. Res.* **2011**, *380*, 173–178. [CrossRef]
64. *TAPPI T-830*; Ink Rub Test of Container Board and Corrugated Board. Technical Association of the Pulp and Paper Industry (TAPPI): Atlanta, GA, USA, 2018.
65. Sonmez, S.; Salam, A.; Fleming, P.D.; Pekarovicova, A.; Wu, Q. Usability of Cellulose-Based Binder in Water-Based Flexographic Ink. *Color. Technol.* **2023**, *139*, 239–247. [CrossRef]
66. Roffey, C. Ultraviolet Curing for Offset Printing Inks, and Varnishes. *J. Oil Colour Chem. Assoc.* **1986**, *69*, 288–296.
67. Shukla, V.; Bajpai, M.; Singh, D.K.; Singh, M.; Shukla, R. Review of Basic Chemistry of UV-Curing Technology. *Pigment Resin Technol.* **2004**, *33*, 272–279. [CrossRef]